Ab Initio Modelling of Photoinduced Electron Dynamics in Nanostructures

A Thesis

Presented Upon Application for
Admission to the Degree of

Doctor of Philosophy

in the
Faculty of Engineering and Physical Sciences

by

Ryan J. McMillan
MSci (Hons) 2013

School of Mathematics and Physics
Queen's University Belfast
Northern Ireland

July 2016

Contents

List of Figures

Chapter 1

Background and Introduction

1.1 Motivation - Solar Technology

1.2 2D Materials in Photonics

1.3 Increasing Light Absorption in 2D Materials

Chapter 2

Theory

2.1 Background Theory

2.1.1 Electronic Structure Calculations

2.1.2 Excited State Calculations

2.1.3 Obtaining Optical Properties

2.2 Projected Equations of Motion (PEOM) Method for Semiconductor-Metal Composites

The efficiency of a PV device is largely determined by its ability to absorb light. We mentioned in Section 1.3 that the performance of 2D, TMD-based solar cells may be improved by depositing MNPs on the TMD monolayer. In the presence of light, the MNPs enhance the field near the monolayer which in turn increases its light absorption.

The absorption in the monolayer may be obtained theoretically using the methods described in Section 2.1. For example, to calculate the absorption in a monolayer of MoS_2, one would first perform a DFT calculation on a unit cell (containing three atoms) to determine the ground state electronic configuration. A linear response TDDFT calculation could then be carried out and the optical absorption spectrum obtained. Such calculations are routine and can be easily completed on a modern desktop computer in a relatively short period of time. Suppose we now wish to perform a similar calculation for an MoS_2 monolayer decorated with gold nanoparticles of diameter 15 nm, similar to the system studied experimentally in Ref. [1]. In this case, one must construct a supercell containing around 50 000 times more atoms and having a volume greater than 100 000 times that of the original unit

cell of the bare MoS_2 monolayer. Such a calculation at the DFT level would prove extremely demanding: even with a linearly scaling code running on many cores of a supercomputer, the boundaries on computational resources are being pushed if not exceeded. Moreover, the calculation becomes infeasible if one wishes to model excitonic effects using, for example, the Bethe-Salpeter Equation as described in Section 2.1.

For this system, however, we are interested primarily with the optical response of the MoS_2 monolayer as it is the 'active' component of the PV device. The MNP on the other hand contributes just to modify the optical properties of the monolayer. Due to the large difference in scale of the MNP compared to the monolayer (in terms of the unit cells required for the DFT calculations), it may then be appropriate to model the MNP on a level of theory less computationally demanding than DFT and to couple the dynamics to those of the monolayer by some effective method.

Indeed, similar problems occur in other areas of computational chemistry and various hybrid methods have been used to great effect over the past few decades. For example, the quantum mechanics/molecular mechanics (QM/MM) approach has been widely applied to study chemical reactions in large systems. In the QM/MM method, the larger environment (e.g. a solvent) is treated on the basis of classical molecular mechanics while the smaller system of interest (e.g. a molecule) is treated using a quantum approach (e.g. DFT). The two systems can then be coupled via force fields or electrostatically as in the polarizable continuum model.

In Ref. [2] a method is developed for modelling the interaction between a semiconducting quantum dot (SQD) and an MNP under illumination. In this case, the SQD is treated as a two-level atomic-like system using the density matrix formalism of quantum mechanics while the MNP is modelled using classical electrodynamics. The dynamics of the two systems are then coupled through the externally applied field using a dipole-dipole approximation. The dynamics of this hybrid complex can be solved analytically within the so-called rotating wave approximation (RWA) as described in detail in Appendix A. This analytical solution is valid provided the applied field is a slowly-varying monochromatic pulse of frequency close to the frequency gap of the SQD. Moreover, the optical response function of the MNP is assumed to be much broader than that of the SQD which is inherently narrow due to its two-level nature and relatively long dephasing times. As it stands, the solution will not hold for ultrafast pulse excitation which is an area of current interest for such systems. Moreover, if the SQD is replaced with a semiconducting monolayer, the two-level quantum description will not suffice and the profile of the MNP response function can no longer be considered 'broad'. Therefore, the method should be generalised to lift the restrictive approximations commonly used, giving rise to the proposed project equations of motion (PEOM) approach described in this section.

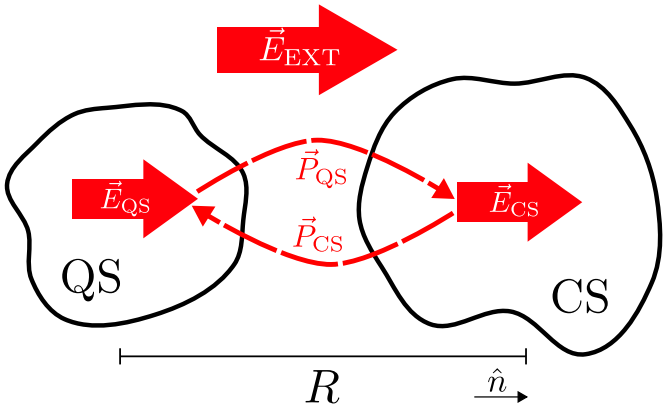

Figure 2.1: Schematic diagram showing the dipole-dipole interaction between a QS and a CS, separated by a distance R. When an external field, $\vec{E}_{\mathsf{EXT}}$, is applied, a dipole moment, $\vec{P}_{\mathsf{QS}}$, is induced in the QS, generating a field. The CS thus experiences this dipole field in addition to the external field, and we denote the total field felt by the CS as $\vec{E}_{\mathsf{CS}}$. Similarly, due to $\vec{E}_{\mathsf{CS}}$, a dipole field is generated in the CS which is in turn felt by the QS in addition to $\vec{E}_{\mathsf{EXT}}$, and we denote the total field felt by the QS as $\vec{E}_{\mathsf{QS}}$. In this way, the QS and CS dynamics are coupled through the external field.

[Would the terms "primary system" and "auxiliary system" describe the setup better?] In order to introduce the PEOM method, we consider a general composite comprising two, isolated subsystems in a vacuum: a larger system to be treated classically—the classical system (CS)—and a smaller system of interest to be treated on the basis of quantum mechanics—the quantum system (QS). For example, in the semiconducting monolayer-MNP system, the monolayer would be the QS and the MNP the CS. The QS and CS shall be separated by some distance, R. An external field, $\vec{E}_{\mathrm{EXT}}(t)$, is applied which induces a dipole-dipole interaction between the two systems as described in Fig. 2.1. To simplify the notation, we assume that the QS and CS are isotropic media. For the generalization to the anisotropic case see Appendix B.1. We write $\vec{E}_{\mathrm{EXT}}(t) \equiv E_{\mathrm{EXT}}(t)\hat{e}$ and denote the unit vector pointing along the line separating the centres of the systems as $\hat{n}$. The fields felt by the QS and CS are then, respectively **[?, ?, ?]**, (note that I've removed the background dielectric constant, , as I only ever use a vacuum and it simplifies notation.)

$$\vec{E}_{\mathrm{QS}}(t) = E_{\mathrm{EXT}}(t)\hat{e} + \frac{P_{\mathrm{CS}}(t)}{R^3}\vec{g}\,, \tag{2.1a}$$

$$\vec{E}_{\mathrm{CS}}(t) = E_{\mathrm{EXT}}(t)\hat{e} + \frac{P_{\mathrm{QS}}(t)}{R^3}\vec{g}\,, \tag{2.1b}$$

where $P_{\mathrm{CS}}(t)$ ($P_{\mathrm{QS}}(t)$) is the total dipole moment of the CS (QS), and

$$\vec{g} = 3\hat{n}\,(\hat{e}\cdot\hat{n}) - \hat{e}\,. \tag{2.2}$$

Is this actually correct? I can see that if $\hat{n}$ is parallel or perpendicular to $\hat{e}$ then yes, but what

if it's at 45 degrees? Will there be a dipole along $\hat{e}$ and $\hat{n}$ both?...

The time-dependent dipole moment of the QS, $P_{\mathrm{QS}}(t)$, can be obtained, e.g., using the methods outlined in Section REF. In general, it is found by solving some equations of motion, whether they be from the density matrix master equation (Eq. REF), or the real-time Bethe-Salpeter equation (Eq. REF), although the theory presented here is independent of the chosen method.

For the CS, rather than calculate the dipole moment explicitly by solving EOMs from quantum theory (or even from classical electrodynamics), we assume that its frequency dependent polarizability, $\alpha(\omega)$, is already known. This may have been previously obtained, however, from *ab-initio* calculations similar to the QS, or from experimental data or classical approximations. Its dipole moment can then be described (in the linear response regime) via [1]

$$\vec{P}_{\mathrm{CS}}(\omega) = \alpha(\omega)\vec{E}_{\mathrm{CS}}(\omega) \ . \tag{2.3}$$

In the time domain, however, the dipole moment is written in terms of the response function $\alpha(t)$, as

$$\vec{P}_{\mathrm{CS}}(t) = \int_{-\infty}^{t} \alpha(t-t')\vec{E}_{\mathrm{CS}}(t')dt' \ . \tag{2.4}$$

Now, the EOMs that determine $\vec{P}_{\mathrm{QS}}(t)$ depend on $\vec{E}_{\mathrm{QS}}(t)$ which in turn depends on $\vec{P}_{\mathrm{CS}}(t)$ from Eq. (2.1a). They are generally solved using an iterative algorithm, such as the fourth-order Runge-Kutta method (see Appendix C –not sure whether it's necessary to include this in the appendix...), where the time domain is split into a set of discrete points. However, computing the integral in Eq. (2.4) at each time-step in the solution is cumbersome and the values of $\vec{E}_{\mathrm{CS}}(t)$ and $\alpha(t)$ for each time-step must be held in memory which may not be feasible for long simulations. Moreover, while $\alpha(\omega)$ is known beforehand, $\alpha(t)$ is not and would have to be calculated using, e.g., a discrete fourier transform. In this case one would have to ensure a sufficiently large (small?) time-resolution of the transform in order to match the time-step in the algorithm used to solve the quantum EOMs. However, the resolution is limited to whatever data is available for $\alpha(\omega)$. Not sure if this last part is necessary, or too confusing. Also, would this method actually work? I would guess a very small time-step would be needed...

In Ref. [**?**], a method (originally devised for memory kernels in the Generalised Langevin Equation) is presented for avoiding the memory-dependent time-convolution inherent in Eq. (2.4). Inspired by this, we introduce N complex auxiliary degrees of freedom, $\{\vec{s}_k(t)\}$

[1] Gaussian units are assumed throughout this thesis –THIS SHOULD GO AT THE START SOMEWHERE INSTEAD.

which satisfy the following projected equations of motion (PEOMs)

$$\dot{\vec{s}}_k = -(\gamma_k + \mathrm{i}\omega_k)\,\vec{s}_k + \mathrm{i}\vec{E}_{\mathrm{CS}}(t) \quad \text{for } k = 1, 2, \ldots, N\ . \tag{2.5}$$

We then state that $\vec{P}_{\mathrm{CS}}(t)$ can be written as

$$\vec{P}_{\mathrm{CS}}(t) \approx \sum_{k=1}^{N} c_k \mathrm{Re}\left[\vec{s}_k(t)\right]\ , \tag{2.6}$$

so that the memory-dependent integral in Eq. (2.4) is replaced with an expansion over the functions $\vec{s}_k$ found by solving the differential equations in Eq. (2.5). As these differential equations no longer contain a time-convolution (i.e., they are "memoryless"), they can be efficiently integrated using, e.g., the same iterative algorithm as for the QS. Therefore, the QS EOMs and the CS PEOMs can be efficiently solved in a coupled fashion. All that is required is to find suitable values for the (real) parameters $\{c_k, \gamma_k, \omega_k\}$ in Eq. (2.5). The formal solution of Eq. (2.5) is

$$\vec{s}_k(t) = \int_{-\infty}^{t} \mathrm{i}\, e^{-(\gamma_k + \mathrm{i}\omega_k)(t-t')}\vec{E}_{\mathrm{CS}}(t')dt'\ . \tag{2.7}$$

Substituting the real part of Eq. (2.7) into Eq. (2.6) and rearranging yields

$$\vec{P}_{\mathrm{CS}}(t) \approx \int_{-\infty}^{t} \left(\sum_{k=1}^{N} c_k e^{-\gamma_k(t-t')}\sin[\omega_k(t-t')]\right)\vec{E}_{\mathrm{CS}}(t')dt'\ , \tag{2.8}$$

and comparing with Eq. (2.4) we see that

$$\alpha(t) \approx \sum_{k=1}^{N} c_k e^{-\gamma_k t}\sin(\omega_k t)\ . \tag{2.9}$$

Taking the Fourier transform of Eq. (2.9) (using the causality condition) gives

$$\alpha(\omega) \approx \sum_{k=1}^{N} \frac{c_k}{2}\left[\frac{1}{\omega + \omega_k + \mathrm{i}\gamma_k} - \frac{1}{\omega - \omega_k + \mathrm{i}\gamma_k}\right]\ . \tag{2.10}$$

Hence, the parameters $\{c_k, \gamma_k, \omega_k\}$ may be found by fitting the frequency-dependent polarizability of the CS (which is known) to the functions on the RHS of Eq. (2.10) (e.g. using the least squares method–in appendix?).

Chapter 3

Results

3.1 Semiconducting Quantum Dot-Metal Nanoparticle Hybrid

In order to test the proposed PEOM method detailed in Section 2.2, we model a semiconducting quantum dot (SQD) as the quantum (primary) system and a metal nanoparticle (MNP) as the classical (auxiliary) system. The SQD-MNP hybrid system has been studied extensively both theoretically (REFS) and experimentally (REFS). In particular, in Ref. [2], Zhang et al. introduce a simple theoretical model in which the SQD is treated as a two-level, atomic-like quantum system whose dynamics are solved using the density matrix formalism of quantum mechanics. The MNP on the other hand is treated classically and the systems' dynamics are coupled through the external field. Indeed, this method provided the basis for the PEOM method.

For a monochromatic external field, the energy absorption rate of the hybrid system can be calculated analytically by means of the rotating wave approximation (RWA). In Section 3.1.4, we compare examples of these analytical solutions and show agreement with the PEOM method.

For a pulsed external field, population inversion in the SQD can be obtained and modified by the presence of the MNP. For slowly-varying pulse envelopes, the density matrix equations of motion for the SQD can be solved semi-analytically within the RWA and in Section 3.1.5, we show agreement with the PEOM method for picosecond pulses. However, in the case of ultrafast, femtosecond pulses, we show that the RWA breaks down and the PEOM method must be preferred for more accurate results.

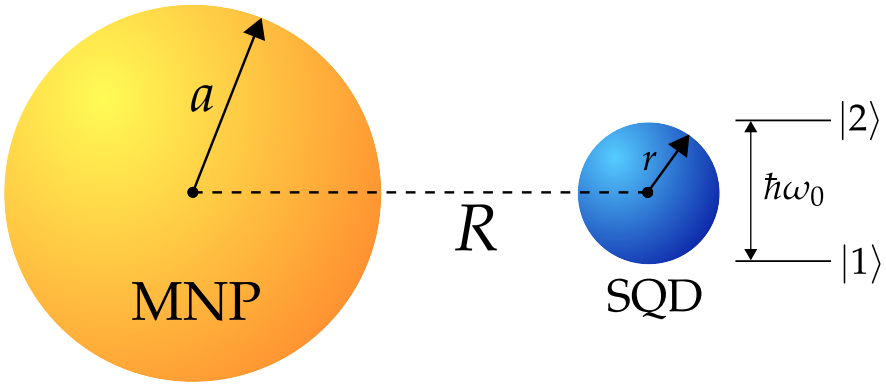

Figure 3.1: Schematic diagram of a spherical metal nanoparticle (MNP) of radius, a, separated by a distance, R, from a spherical semiconducting quantum dot (SQD) of radius, r. The MNP is modelled classically while the SQD is treated as a two-level quantum system with ground state, $|1\rangle$, and excited state, $|2\rangle$, separated by an energy gap of $\hbar\omega_0$.

3.1.1 Describing the System

Consider a spherical, gold MNP of radius, a, separated by a distance, R, from a spherical SQD of radius, r, as shown in Fig. 3.1. From Eq. (2.1), when an external field $E_{\text{EXT}}(t)$ is applied, the fields felt by the SQD and MNP are, respectively,

$$E_{\text{SQD}}(t) = E_{\text{EXT}}(t) + g\frac{P_{\text{MNP}}(t)}{R^3}\,, \tag{3.1}$$

$$E_{\text{MNP}}(t) = E_{\text{EXT}}(t) + g\frac{P_{\text{SQD}}(t)}{R^3}\,, \tag{3.2}$$

where $P_{\text{SQD}}(t)$ ($P_{\text{MNP}}(t)$) is the dipole moment of the SQD (MNP). We have taken the external field to be polarized along the line connecting the centres of the particles so that $\hat{n} = \hat{e}$. From Eq. (2.2), we have that $\vec{g} = 2\hat{e}$ and so all fields are pointing in the direction of the external field, $\hat{e}$, allowing us to drop the vector notation.

The SQD is treated as a 2-level, atomic-like system with ground state, $|1\rangle$, and excited state, $|2\rangle$, separated by an energy gap of $\hbar\omega_0$ (ω_0 is known as the exciton frequency). We use the density matrix formalism so that the SQD can be described by a 2×2 density matrix, $\boldsymbol{\rho}(t)$, whose elements can be written as (see Appendix REF(–from differentiation))

$$\begin{cases} \dot{\Delta} &= -\frac{4\tilde{\mu}_{21}}{\hbar}E_{\text{SQD}}(t)\text{Im}\left[\rho_{21}\right] - \Gamma_{11}(\Delta - 1) \\ \dot{\rho}_{21} &= -\left(\Gamma_{21} + \mathrm{i}\omega_0\right)\rho_{21} + \mathrm{i}\frac{\tilde{\mu}_{21}}{\hbar}E_{\text{SQD}}(t)\Delta \end{cases}\,, \tag{3.3}$$

where $\Delta(t) = \rho_{11}(t) - \rho_{22}(t)$ is the population difference between the ground and excited states, and $\rho_{12} = \rho_{21}^*$. Γ_{11} and Γ_{21} are the population decay and dephasing rates of the system respectively. The SQD is assumed to be a dielectric sphere with dielectric constant ϵ_{S} and so

it has a screened dipole matrix element,

$$\tilde{\mu}_{21} = \frac{\mu_{21}}{\epsilon_{\text{effS}}} , \tag{3.4}$$

where μ_{21} is the bare dipole matrix element and [?]

$$\epsilon_{\text{effS}} = \frac{2+\epsilon_S}{3} . \tag{3.5}$$

(Not sure if these should go here or later...) We take the SQD system parameters from Ref. [?], which are typical of a CdSe quantum dot. The dielectric constant is taken to be $\epsilon_S = 6$ with (bare) transition dipole moment $\mu = 0.65e$ nm and exciton energy $\hbar\omega_0 = 2.5$ eV close to the plasmon peak of the gold MNP. The decay and dephasing times are given by $\Gamma_{11}^{-1} = 0.8$ ns and $\Gamma_{21}^{-1} = 0.3$ ns.

The dipole moment of the SQD is

$$P_{\text{SQD}}(t) = \text{tr}\left(\boldsymbol{\rho}\boldsymbol{\mu}\right) \tag{3.6}$$

$$= \tilde{\mu}_{21}\left(\rho_{12} + \rho_{21}\right), \tag{3.7}$$

where $\text{tr}\left(\cdots\right)$ is the matrix trace operator. The dipole moment of the MNP is taken to be

$$P_{\text{MNP}}(\omega) = \alpha_{\text{MNP}}(\omega) E_{\text{MNP}}(\omega) , \tag{3.8}$$

where $\alpha_{\text{MNP}}(\omega)$ is the frequency-dependent polarizability. For comparison with previous literature, we approximate $\alpha_{\text{MNP}}(\omega)$ by the Clausius-Mossotti formula,

$$\alpha_{\text{MNP}}(\omega) = a^3 \frac{\epsilon_M(\omega) - 1}{\epsilon_M(\omega) + 2} , \tag{3.9}$$

where $\epsilon_M(\omega)$ is the frequency-dependent dielectric function of the bulk metal [?] (we use the analytical model for bulk gold as given by Etchegoin et al. [?]).

For the external field, we shall consider the following light pulse,

$$E_{\text{EXT}}(t) = f(t) E_0 \cos(\omega_L t) , \tag{3.10}$$

where $f(t)$ is a dimensionless pulse envelope, ω_L is the carrier (or central) frequency and E_0 is the amplitude. The field strength is normally given in terms of the intensity, I_0, by

$$I_0 = \frac{c}{2} E_0^2 , \tag{3.11}$$

where c is the speed of light. $I_0 = \frac{\epsilon_0 c}{2} E_0^2$, in gaussian units, does the ϵ_0 (vacuum permittivity)

just disappear, or should there be a 4π in there?...

To determine the solutions to Eq. (3.3), one can (i) follow the PEOM method in Section 2.2, or (ii) use analytical approximations. We shall now describe both procedures.

3.1.2 Solution within the PEOM Method

In the PEOM method, we approximate the time-dependent dipole moment of the MNP by

$$P_{\mathrm{MNP}}(t) \approx \sum_{k=1}^{N} c_k \mathrm{Re}\left[s_k(t)\right] \ , \tag{3.12}$$

where the functions, $\{s_k\}$, are found by solving the differential equations,

$$\dot{s}_k = -\left(\gamma_k + \mathrm{i}\omega_k\right) s_k + \mathrm{i}E_{\mathrm{MNP}}(t) \quad \text{for } k = 1, 2, \ldots, N \ . \tag{3.13}$$

The first step in the implementation, therefore, is to determine the paramters, $\{c_k, \omega_k, \gamma_k\}$, by fitting the frequency-dependent polarizability of the MNP, $\alpha_{\mathrm{MNP}}(\omega)$, to

$$\alpha_{\mathrm{MNP}}(\omega) \approx \sum_{k=1}^{N} \frac{c_k}{2} \left[\frac{1}{\omega + \omega_k + \mathrm{i}\gamma_k} - \frac{1}{\omega - \omega_k + \mathrm{i}\gamma_k}\right] \ . \tag{3.14}$$

The polarizability for the gold MNP from Eq. (3.9) is shown in Fig. 3.2 along with a least-squares fit to Eq. (3.14) which required $N = 21$ fitting functions in order to get a fit of sufficient accuracy over the range 0–10 eV. The parameters obtained are given in Appendix REF Should I include these in the appendix?.

Once the parameters are known, we can then solve Eq. (3.3) simultaneously with (3.13) using the fourth-order Runge-Kutta method (Appendix C) where at the end of each step $P_{\mathrm{MNP}}(t)$ and $P_{\mathrm{SQD}}(t)$ are updated using Eqs. (3.7) and (3.12) resepectively. (Should I include code/pseudo code of the algorithm in the Appendix?).

3.1.3 Analytical and Semi-Analytical Solutions

To solve Eq. (3.3) analytically, we first separate out the slowly and quickly oscillating terms of the off-diagonal density matrix elements:

$$\rho_{12}(t) = \bar{\rho}_{12}(t) e^{\mathrm{i}\omega_L t} \ , \tag{3.15a}$$

$$\rho_{21}(t) = \bar{\rho}_{21}(t) e^{-\mathrm{i}\omega_L t} \ , \tag{3.15b}$$

where $\bar{\rho}_{12}(t)$ and $\bar{\rho}_{21}(t)$ are assumed to vary much larger timescale than $2\pi/\omega_L$. We assume a *slowly-varying* pulse envelope so that $f(t)$ also varies on a timescale larger that $2\pi/\omega_L$. Thus,

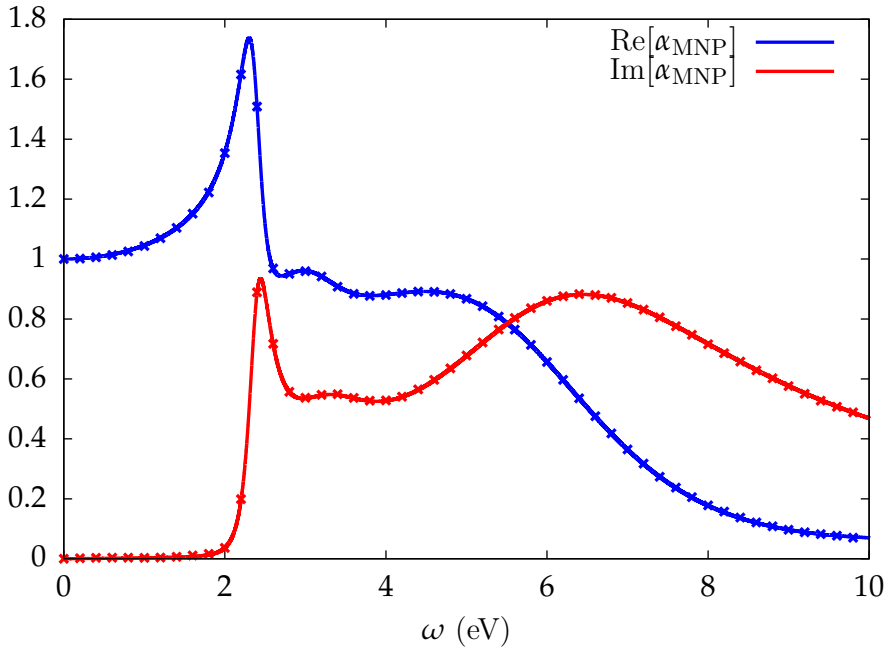

Figure 3.2: Real (solid blue) and imaginary (solid red) parts of the MNP frequency-dependent polarizability, $\alpha_{\mathrm{MNP}}(\omega)$, as given by Eq. (3.9). The least-squares fit is shown as crosses, obtained from Eq. (3.14) with $N = 21$. The units of the y-axis are in $1/a^3$ where a is the radius of the MNP.

from Eq. (3.1), we can express the field felt by the SQD approximately as (see Appendix REF)

$$E_{\mathrm{SQD}}^{(\mathrm{eff})}(t) = \frac{\hbar}{\tilde{\mu}_{21}}\left[\left(\frac{\Omega(t)}{2}e^{-\mathrm{i}\omega_L t} + G\rho_{21}(t)\right) + \mathrm{c.c.}\right], \tag{3.16}$$

where

$$\Omega(t) = f(t)\Omega_{\mathrm{eff}}\,, \tag{3.17a}$$

$$\Omega_{\mathrm{eff}} = \Omega_0\left[1 + \frac{g}{R^3}\alpha_{\mathrm{MNP}}(\omega_L)\right]\,, \tag{3.17b}$$

$$G = \frac{g^2\tilde{\mu}_{21}^2}{\hbar R^6}\alpha_{\mathrm{MNP}}(\omega_L)\,, \tag{3.17c}$$

where

$$\Omega_0 = \tilde{\mu}_{21}E_0/\hbar \tag{3.18}$$

is the Rabi frequency of the isolated SQD.

One may then substitute Eq. (3.16) into the density matrix EOMs in Eq. (3.3) and determine a numerical solution (e.g. using the fourth-order Runge-Kutta method). This is equivalent to the method used by Yang et al. in REF. Alternatively, one can make use of the rotating wave approximation (RWA) which assumes that the carrier frequency is close to resonant with the exciton frequency ($\omega_L \approx \omega_0$) so that terms oscillating at frequencies far from ω_0 can

be neglected. By substituting Eq. (3.16) into Eq. (3.3) and employing the RWA, one arrives at the following, modified RWA EOMs for the density matrix (see Appendix REF)

$$\begin{cases} \dot{\Delta} & = 4\mathrm{Im}\left[\left(\frac{\Omega}{2}+G\bar{\rho}_{21}\right)\bar{\rho}_{12}\right]+\Gamma_{11}\left(1-\Delta\right) \\ \dot{\bar{\rho}}_{21} & = \left[\mathrm{i}\left(\omega_L-\omega_0+G\Delta\right)-\Gamma_{21}\right]\bar{\rho}_{21}+\mathrm{i}\frac{\Omega}{2}\Delta \end{cases} . \tag{3.19}$$

One can then numerically solve these modified EOMs to determine the dynamics of the slowly-varying parts, $\bar{\rho}_{21}(t)$, which should be similar to the full dynamics of $\rho_{21}(t)$ provided the RWA is valid. This is equivalent to the method used in REFs.

In the case of a rectangular envelope of unitary height ($f(t) = 1$), i.e. a monochromatic wave,

$$E_{\mathrm{EXT}}(t) = E_0 \cos(\omega_L t) \, , \tag{3.20}$$

Eq. (3.19) may be solved analytically under the steady-state conditions $\dot{\Delta} = \dot{\bar{\rho}}_{21} = 0$ to obtain

$$\bar{\rho}_{21}^{\mathrm{s.s.}} = \frac{-\Omega_{\mathrm{eff}}\Delta^{\mathrm{s.s.}}}{\omega_L-\omega_0+G\Delta^{\mathrm{s.s.}}+\mathrm{i}\Gamma_{21}}, \tag{3.21}$$

where $\Delta^{\mathrm{s.s.}}$ is found by solving a cubic equation (see Appendix REF).

Eq. (3.22) allows us to calculate the energy absorption rate of the system, while we can investigate population inversion by solving the density matrix EOMs directly.

3.1.4 Energy Absorption Rates

The energy absorption rate (EAR) of the SQD-MNP system is a steady-state property in response to the monochromatic wave given in Eq. (3.20). Suppose a steady-state is achieved (i.e. $\dot{\Delta} = \dot{\bar{\rho}}_{21} = 0$) at $t = T^{\mathrm{s.s}}$. Then we define

$$\Delta^{\mathrm{s.s.}} = \Delta\left(T^{\mathrm{s.s}}\right) \, , \tag{3.22a}$$

$$\bar{\rho}_{21}^{\mathrm{s.s.}} = \bar{\rho}_{21}\left(T^{\mathrm{s.s}}\right) \, . \tag{3.22b}$$

The EAR of the SQD is defined as

$$Q_{\mathrm{SQD}} = \frac{1}{2}\hbar\omega_0\Gamma_{11}\left(1-\Delta^{\mathrm{s.s.}}\right) \, , \tag{3.23}$$

while that of the MNP is

$$Q_{\mathrm{MNP}} = \left\langle \int \boldsymbol{j}\left(T^{\mathrm{s.s.}}\right)\cdot\boldsymbol{E}_{\mathrm{MNP}}^{(\mathrm{in})}\left(T^{s.s}\right)dV \right\rangle \, , \tag{3.24}$$

where

$$j(t) = \frac{1}{V}\frac{d}{dt}P_{\text{MNP}}(t) \tag{3.25}$$

is the current density in the MNP [?](is this the correct formula for current density?) and $E^{(\text{in})}_{\text{MNP}}(t)$ is the field inside the MNP. For a sphere it can be shown that [?]

$$E^{(\text{in})}_{\text{MNP}}(t) = E_{\text{MNP}}(t) - \frac{4}{3}\pi P_{\text{MNP}}(t)\ . \tag{3.26}$$

We define the time-average of a function $h(t)$ as

$$\langle h(t)\rangle \equiv \frac{1}{\delta T}\int_t^{t+\delta T} h(t')dt'\ , \tag{3.27}$$

and choose δ_t to be one period of the wave,

$$\delta t = \frac{2\pi}{\omega_L}\ . \tag{3.28}$$

(i) Solution in the PEOM

In the PEOM solution (see Section 3.1.2), $\Delta(t)$ is found by numerically solving Eq. (3.3) and so $\Delta^{\text{s.s.}}$, and therefore Q_{SQD} (Eq. (3.23)), can be calculated trivially assuming the simulation time is long enough that a steady-state can be said to have been reached.

To calculate Q_{MNP} from Eq. (3.24), one must first calculate the current density from Eq. (3.25). The derivative, $\delta/\delta t P_{\text{MNP}}(t)$, may be calculated numerically though it can be shown from Eqs. (3.12) and (3.13) (see Appendix REF) that

$$\frac{dP_{\text{MNP}}}{dt} = \sum_{k=1}^{N} c_k\left(\omega_k \text{Im}\left[s_k(t)\right] - \gamma_k \text{Re}\left[s_k(t)\right]\right)\ . \tag{3.29}$$

The time-average in Eq. (3.24) can then be found by numerical integration. For a small time-step, h, in the fourth order Runge-Kutta method, we found the crude approximation,

$$\int_{t_n}^{t_m} f(t')dt' \approx h\sum_{i=n}^{m} f(t_i)\ , \tag{3.30}$$

to be sufficient.

(ii) Analytical Solution

As mentioned in Section 3.1.3, $\Delta^{\text{s.s.}}$, and therefore Q_{SQD}, can be found analytically by solving Eq. (3.3) within the RWA.

Within the RWA, it can be shown that field felt by the MNP and its polarization are given, respectively, by (see Appendix REF)

$$E_{\text{MNP}}(t) = \bar{E}_{\text{MNP}}(t)e^{-i\omega_L t} + \text{c.c.}\,, \tag{3.31}$$

$$P_{\text{MNP}}(t) = \alpha_{\text{MNP}}(\omega_L)\bar{E}_{\text{MNP}}(t)e^{-i\omega_L t} + \text{c.c.}\,, \tag{3.32}$$

where

$$\bar{E}_{\text{MNP}}(t) = \frac{E_0}{2} + \frac{g\tilde{\mu}_{21}}{R^3}\bar{\rho}_{21}(t)\,. \tag{3.33}$$

If we substitute (**??**) into Eq. (3.24) and assume then using the RWA yields the following (see Appendix REF),

$$Q_{\text{MNP}} = 2\omega_L \text{Im}\left[\alpha_{\text{MNP}}(\omega_L)\right]\left|\frac{E_0}{2} + \frac{g\tilde{\mu}_{21}}{R^3}\bar{\rho}_{21}^{\text{s.s.}}\right|^2\,. \tag{3.34}$$

3.1.5 Population Inversion

Copy section from paper, leaving out the EOMs as they are in the previous section. Explain more about how E_0 comes about from rearranging the pulse area.

3.2 Optical Spectra for MoS_2 Composites

Appendix A

Semiconducting Quantum Dot-Metal Nanoparticle Hybrid: Solution within the Rotating Wave Approximation

Appendix B

The Projected Equations of Motion Method

B.1 Generalization to Anisotropic Media

In the case of anisotropic media, the effective fields in Eq. (2.1) become

$$\vec{E}_{\mathrm{QS}}(t) = \vec{E}_{\mathrm{EXT}}(t) + \frac{3\hat{n}\left(\vec{P}_{\mathrm{CS}}(t)\cdot\hat{n}\right) - \vec{P}_{\mathrm{CS}}(t)}{R^3}\,, \tag{B.1}$$

$$\vec{E}_{\mathrm{CS}}(t) = \vec{E}_{\mathrm{EXT}}(t) + \frac{3\hat{n}\left(\vec{P}_{\mathrm{QS}}(t)\cdot\hat{n}\right) - \vec{P}_{\mathrm{QS}}(t)}{R^3}\,, \tag{B.2}$$

and the polarizability of the classical system now becomes a tensor

$$\boldsymbol{\alpha} = \begin{pmatrix} \alpha^{(xx)} & \alpha^{(xy)} & \alpha^{(xz)} \\ \alpha^{(yx)} & \alpha^{(yy)} & \alpha^{(yz)} \\ \alpha^{(zx)} & \alpha^{(zy)} & \alpha^{(zz)} \end{pmatrix}\,, \tag{B.3}$$

The theory then proceeds as in Section 2.2 except in how $\vec{P}_{\mathrm{CS}}(t)$ is expanded: we expand the i-th vector component ($i = x, y, z$) as

$$P^{(i)}_{\mathrm{CS}}(t) = \sum_{j=x,y,z}\sum_{k=1}^{N_{ij}} c_k^{(ij)}\,\mathrm{Re}\left[s_k^{(ij)}(t)\right]\,, \tag{B.4}$$

where the functions $s_k^{(ij)}(t)$ are found from the differential equations

$$\dot{s}_k^{(ij)} = -\left(\gamma_k^{(ij)} + \mathrm{i}\omega_k^{(ij)}\right) s_k^{(ij)} + \mathrm{i}E^{(i)}_{\mathrm{CS}}(t)\,, \tag{B.5}$$

for $i, j = x, y, z$ and $k = 1, \ldots, N_{ij}$ and the parameters are found by fitting each component of the $\boldsymbol{\alpha}$ tensor to

$$\alpha^{(ij)}(\omega) = \sum_{k=1}^{N_{ij}} c_k^{(ij)} \left[\frac{1}{(\omega_k^{(ij)} - \omega) - \mathrm{i}\gamma_k^{(ij)}} + \frac{1}{(\omega_k^{(ij)} + \omega) + \mathrm{i}\gamma_k^{(ij)}} \right] , \tag{B.6}$$

for $i, j = x, y, z$.

Appendix C

Fourth-Order Runge-Kutta Method for Solving First-Order ODEs

Suppose we have a first-order differential equation of the form

$$\dot{y} = f(t, y) \,, \tag{C.1}$$

where $y \equiv y(t)$, and we want to approximate the solution over some interval $t \in [a, b]$ ($b > a$). We begin by splitting the interval into $N + 1$ equally-spaced points, $\{t_0, t_1, \ldots, t_N\}$ with $t_0 = a$ and $t_N = b$, such that

$$t_n = a + nh \,, \qquad n = 0, 1, \ldots, N \,, \tag{C.2}$$

where h is the spacing, or step-size, given by

$$h = \frac{b - a}{N} \,. \tag{C.3}$$

Provided $y(t_0) = y(a)$ (the initial condition) is known, the fourth-order Runge-Kutta method approximates $\{y(t_1), y(t_2), \ldots y(t_N)\}$ using the following algorithm: **[?]**

For $n = 0, 1, \ldots, N-1$,

$$k_1 = h\ f(t_n, y_n)\ ,$$
$$k_2 = h\ f\left(t_n + \frac{1}{2}h, y_n + \frac{1}{2}k_1\right)\ ,$$
$$k_3 = h\ f\left(t_n + \frac{1}{2}h, y_n + \frac{1}{2}k_2\right)\ ,$$
$$k_4 = h\ f(t_n + h, y_n + k_3)\ ;$$
$$y_{n+1} = y_n + \frac{1}{6}(k_1 + 2k_2 + 2k_3 + k_4)\ ;$$
$$t_{n+1} = t_n + h\ .$$

where we have defined

$$y_n \equiv y(t_n)\ .$$

Bibliography

[1] Jiadan Lin, Hai Li, Hua Zhang, and Wei Chen. Plasmonic enhancement of photocurrent in MoS2 field-effect-transistor. *Appl. Phys. Lett.*, 102(20):203109, 2013.

[2] Wei Zhang, Alexander O. Govorov, and Garnett W. Bryant. Semiconductor-metal nanoparticle molecules: Hybrid excitons and the nonlinear fano effect. *Phys. Rev. Lett.*, 97(14), 2006.